ELSEVIER

Nuclear Instruments and Methods in Physics Research B 180 (2001) 257–264

NIM B
Beam Interactions with Materials & Atoms

www.elsevier.nl/locate/nimb

Atomistic simulations of point defects in ZrNi intermetallic compounds

C.S. Moura [a,b,*], A.T. Motta [b], N.Q. Lam [c], L. Amaral [a]

[a] *Instituto de Física, Universidade Federal do Rio Grande do Sul, Porto Alegre, Brazil*
[b] *Department of Mechanical and Nuclear Engineering, The Pennsylvania State University, University Park, PA 16802, USA*
[c] *Materials Science Division, Argonne National Laboratory, Argonne, IL 60439, USA*

Abstract

The properties of point defects, including stable configurations, formation and migration energies, and migration mechanisms, in the ZrNi and Zr_2Ni intermetallic compounds were simulated using molecular dynamics and statics, in conjunction with interatomic potentials derived from the Embedded Atom Method. We describe a method to calculate the formation energy of point defects from the program and apply the method to ZrNi and Zr_2Ni. The results showed that vacancies are most stable in the Ni sublattice, with formation energy of 0.83 and 0.61 eV in ZrNi and Zr_2Ni, respectively. Zr vacancies are unstable in both compounds; they spontaneously decay to pairs of Ni vacancy and antisite defect. The interstitial configurations and formation energies were also calculated, with similar behaviors. In ZrNi, vacancy migration occurs preferentially in the [0 2 5] and [1 0 0] directions, with migration energy of 0.67 and 0.73 eV, respectively, and is essentially a two-dimensional process, in the (0 0 1) plane. In Zr_2Ni, vacancy migration is one-dimensional, occurring in the [0 0 1] direction, with a migration energy of 0.67 eV. In both compounds, the presence of Ni antisite defects decreases the Ni vacancy migration energy by up to a factor-of-three, and facilitates three-dimensional motion.

1. Introduction

To understand the irradiation response of ZrNi and Zr_2Ni and their propensity to undergo phase transformations such as chemical disordering and amorphization, it is necessary to have a good knowledge of the properties of point defects in these compounds [1]. Unfortunately, information about point defects is extremely limited for most ordered intermetallics. The aim of the present work is to acquire such knowledge via atomistic simulations. It is also hoped that these computer simulation results would provide guidance to experimental investigations of atomic defects in the compounds, since it is difficult to experimentally distinguish the defects one from the other among the many possible point defect types.

In this study, we performed computer simulations to obtain information about the properties of vacancies and interstitials in the intermetallic compounds ZrNi and Zr_2Ni for which realistic interatomic potentials are available. This infor-

* Corresponding author. Fax: +55-814-865-84-99.
E-mail address: ssm7@psu.edu (C.S. Moura).

0168-583X/01/$ - see front matter
PII: S0168-583X(01)00426-8

mation includes their stable configurations, energetics, and migration mechanisms. The radiation-induced amorphization behavior of these compounds has systematically been investigated, both experimentally and theoretically [2–4].

2. Computational procedure

The computational methods used in the present simulations were molecular statics and molecular dynamics at constant pressure. The simulation cells for ZrNi (orthorhombic, oC8, ζ-BCr-type structure) and Zr_2Ni (body center, tl12, Al_2Cu-type structure) contained 1568 and 1500 atoms, respectively, and were subjected to periodic boundary conditions. The interactions between atoms in the compounds were governed by the potentials which were derived from the Embedded Atom Method (EAM) [5,6] and used in previous studies of defect-induced amorphization [3,4].

The perfect lattice was first equilibrated for 10,000 time steps (25 ps) using molecular dynamics (using a time step of 2.5×10^{-15} s). Then, a vacancy or interstitial was created in a given sublattice near the center of the simulation cell using standard procedures. In the vacancy case, the most stable vacancy configuration could be found simply by relaxing the defective lattice dynamically for another 10,000 time steps. The potential energy of the system was then obtained by a local energy minimization using the Fletcher–Powell scheme, which was proven to be quite efficient [7]. The search for the lowest interstitial energy configuration was, however, carried out by means of simulated annealing [8]: the system was first heated to 800 K for a few hundred time steps, then energy-minimized with the Fletcher–Powell method, and the process was repeated at lower and lower temperatures, down to the desired temperature. For each type of defect, we conducted three runs and took the average value of the energy differences (the variation was less than 0.2%).

For pure elements, given the energies of the perfect lattice and of the lattice containing the defect, the defect formation energy can be readily calculated. In ordered compounds, the formation energies of a Frenkel pair and an antisite pair can be determined in a similar way. However, the calculation of the formation energy of a vacancy or interstitial alone is more complex because the perfect lattice and the lattice with the defect have different chemical compositions [9–11]. We discuss this problem in the following section.

2.1. Calculation of point-defect formation energies

In ordered compounds, the formation of a Frenkel pair (i.e., an atom is removed from a substitutional site and inserted back into a random interstitial site in the lattice) or of an antisite defect pair (i.e., lattice sites of a random pair of atoms of different types are exchanged) does not lead to a deviation from stoichiometry. However, the creation of a vacancy (permanently removing an atom from its substitutional site) or an interstitial (inserting an extra atom into the material) results in a departure from stoichiometry, which must be taken into consideration in the calculation of the defect formation energies.

Let us consider an ordered compound A_zB_y. The chemical potential of A, μ^A, is defined as the change in the Gibbs free energy, G, with respect to the concentration of element A, n^A, at constant temperature, T, pressure, P, and molar fraction of B, n^B,

$$\mu^A = \left(\frac{\partial G}{\partial n^A}\right)_{P,T,n^B}. \tag{1}$$

Any change in the chemical composition will cause a variation in the system total energy, relative to the perfectly ordered state. This difference consists of two contributions: the defect formation energy and the change in the Gibbs free energy due to the chemical potential.

In order to determine the effective defect formation energy, E_f, it is necessary to calculate the defect concentration, n_j, for defect j as a function of temperature T. E_f is then given by the slope of the Arrhenius plot [10,11],

$$E_f^j = -k\frac{d[\ln(n_j)]}{d[T^{-1}]}, \tag{2}$$

where j stands for the type of defect (=i for interstitial or v for vacancy) and k is Boltzmann's

constant. The defect formation energy may be temperature-dependent; we assume that this effect is weak and can be disregarded, i.e., the Arrhenius plot is a straight line. The validity of this assumption is verified later.

The concentration n_j is obtained from the numerical solution of a system of nonlinear equations proposed by Foiles and Daw [10] and adapted here to take into account the presence of interstitials and antisites. The total energy, U, of a system of N^{s} atomic sites is given by the perfect-crystal energy, U_0, plus the contributions from different defects (assuming that their concentrations are low enough so that the defects are non-interacting),

$$\frac{U}{N^{\mathrm{s}}} = \frac{U_0}{N^{\mathrm{s}}} + n_{\mathrm{v}}^{A} H_{\mathrm{v}}^{A} + n_{\mathrm{v}}^{B} H_{\mathrm{v}}^{B} + n_{\mathrm{a}}^{A} \mathrm{H}_{\mathrm{a}}^{A} + n_{\mathrm{a}}^{B} H_{\mathrm{a}}^{B} + n_{\mathrm{i}}^{A} H_{\mathrm{i}}^{A} + n_{\mathrm{i}}^{B} H_{\mathrm{i}}^{B}, \tag{3}$$

where n_j^A (n_j^B) is the concentration of defect j (= v, i, a for vacancy, interstitial and antisite defect) on the A sublattice (respectively B sublattice), and H_j^A (H_j^B) is the energy difference between the perfect crystal and the crystal containing a defect j on sublattice A (respectively, B sublattice).

The introduction of defects into the perfect crystal increases the configurational entropy which is defined by [12]

$$\frac{S}{N^{\mathrm{s}}} = m^{A}\left[s\left(\frac{n_{\mathrm{a}}^{B}}{m^{A}}\right) + s\left(\frac{n_{\mathrm{v}}^{A}}{m^{A}}\right) + s\left(\frac{n_{\mathrm{i}}^{A}}{m^{A}}\right)\right] + m^{B}\left[s\left(\frac{n_{\mathrm{a}}^{A}}{m^{B}}\right) + s\left(\frac{n_{\mathrm{v}}^{B}}{m^{B}}\right) + s\left(\frac{n_{\mathrm{i}}^{B}}{m^{B}}\right)\right], \tag{4}$$

where $m^A = z/(z+y)$, $m^B = 1 - m^A$. The equation above is valid when the number of ways that one can arrange the atom in a crystal containing n_{i} interstitials is equivalent to that in a crystal containing n_{v} vacancies. The ideal entropy function s is defined by

$$s(x) = -[x \ln x + (1-x)\ln(1-x)]. \tag{5}$$

The total concentration of A-atoms, n^A, is given by

$$n^{A} = \left(m^{A} - n_{\mathrm{v}}^{A} + n_{\mathrm{a}}^{A} - n_{\mathrm{a}}^{B} + n_{\mathrm{i}}^{A}\right), \tag{6}$$

where n_{v}^A is the concentration of vacancies in the A sublattice, n_{a}^B is the number of A sites occupied by B-atoms, n_{a}^A is the number of B sites occupied by A-atoms, and n_{i}^A is the number of A atoms occupying interstitial positions.

The Grand-Canonical potential is given by

$$\varphi = U - kTS - \mu_A N_A - \mu_B N_B. \tag{7}$$

Inserting Eqs. (3) and (4) into Eq. (7) and minimizing it with respect to each of the defect concentrations n_j^A and n_j^B (j = v, i, a), we arrive at the corresponding expressions for the concentration of each defect type:

$$n_{\mathrm{v}}^{A} = m^{A}\frac{\exp\left[-(H_{\mathrm{v}}^{A} + \mu^{A})/kT\right]}{1 + \exp\left[-(H_{\mathrm{v}}^{A} + \mu^{A})/kT\right]}, \tag{8}$$

$$n_{\mathrm{a}}^{A} = m^{B}\frac{\exp\left[-(H_{\mathrm{a}}^{A} + \mu^{B} - \mu^{A})/kT\right]}{1 + \exp\left[-(H_{\mathrm{a}}^{A} + \mu^{B} - \mu^{A})/kT\right]}, \tag{9}$$

$$n_{\mathrm{i}}^{A} = m^{A}\frac{\exp\left[-(H_{\mathrm{i}}^{A} - \mu^{A})/kT\right]}{1 + \exp\left[-(H_{\mathrm{i}}^{A} - \mu^{A})/kT\right]}. \tag{10}$$

Eqs. (6) and (8)–(10) have their respective counterparts in the other sublattice written by exchanging A and B. The final set of 10 equations to be solved consists of Eqs. (3), (4), (6) and (8)–(10) and the counterparts of Eqs. (6) and (8)–(10), for the B sublattice. This set of equations is solved for the variables n_{v}^A, n_{v}^B, n_{i}^A, n_{i}^B, n_{a}^A, n_{a}^B, N^A, N^B, μ^A and μ^B, with the temperature as a parameter.

2.2. Calculation of vacancy migration energy

The vacancy migration energies were calculated by minimizing the system energy with the jumping atom constrained at various points along the jump path. This procedure consists basically of taking an atom and pushing it into the neighboring vacant site. This move was done in a series of small steps. With a reaction coordinate η defined, the point $r(\eta)$ along the jump path was specified by

$$r(\eta) = r_1 + \eta[r_2 - r_1]. \tag{11}$$

At $r(\eta)$, the "migrating" atom was confined to the plane normal to $(r_2 - r_1)$ while the surrounding atoms were allowed to relax [7,11]. The mapping of the energy barrier for migration, $E(\eta)$, was then obtained by repeating the calculation for different

values of η, and the highest saddle-point energy (i.e., the maximum value of $E(\eta)$ for η in the range $[-1, 1]$) was taken to be the vacancy migration energy, E_v^m. All calculations were carried out for zero temperature.

3. Results and discussion

3.1. Defect formation energies

In both compounds, the vacancy was found to be most stable in the Ni sublattice. Zr vacancies were highly unstable; if a Zr atom was removed from the Zr sublattice to form a Zr vacancy [v(Zr)] a neighboring Ni atom jumped right into the vacancy, giving rise to an Ni vacancy [v(Ni)] and a Zr-antisite defect [Zr(Ni)]. Similarly, Ni interstitials [i(Ni)] were much more stable than their Zr counterparts: the Zr interstitial [i(Zr)] also decayed into an Ni interstitial [i(Ni)] plus a Zr-antisite defect [Zr(Ni)]. The most stable configurations for the interstitial in Zr_2Ni and ZrNi are shown in Fig. 1. In Zr_2Ni, the stable i(Ni) lies on the (0 0 1) plane, in between the nearest out-of-plane Zr atoms, above and below (labeled "1" and "2"). In ZrNi, the stable i(Ni) is also in the same configuration, i.e. it lies on the (0 0 1) plane, with a nearest Zr atom above and below it. For the sake of clarity, atomic distortions around the extra atoms are not shown in the figures.

The temperature-dependent concentrations of vacancies and interstitials were determined from the set of 10 equations described in Section 2.1, using the values of $H_j^k = U_j^k - U_0$ (the energy difference between the crystal containing a defect j on sublattice k and the perfect crystal) given in Table 1. Figs. 2 and 3 show the Arrhenius plots of these concentrations for Zr_2Ni and ZrNi, respectively. We note that the assumption made in Section 2.1 that the formation energy be independent of temperature is confirmed by the constant slopes of the

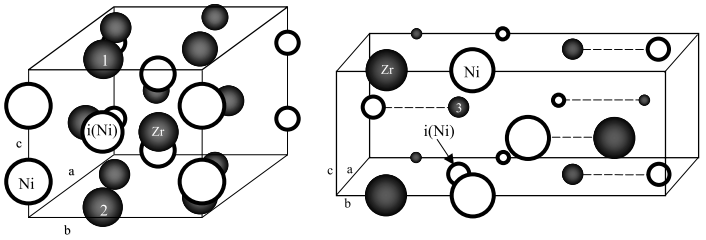

Fig. 1. Interstitial configuration in Zr_2Ni (left) and ZrNi (right). The atom size varies with distance from the front plane.

Table 1
Energy difference H_k^j (in eV) between the perfect crystal and the crystal containing the defect of j-type in the k-sublattice

			Zr_2Ni		ZrNi	
Defect type	k	j	U_j^k	H_j^k	U_j^k	H_j^k
Perfect crystal	–	0	−8836.5481	0	−8884.3336	0
v(Ni)	Ni	v	−8830.7138	5.8343	−8878.5302	5.8034
v(Zr)	Zr	v	−8828.8811	7.6670	−8875.9752	8.3584
i(Ni)	Ni	i	−8839.6712	−3.1231	−8887.6350	−3.3014
i(Zr)	Zr	i	−8839.7573	−3.2092	−8887.9436	−3.6100
Ni(Zr)	Zr	a	−8834.9491	1.5990	−8882.1148	2.2188
Zr(Ni)	Ni	a	−8836.0142	0.5339	−8884.3391	−0.0055
Ni(Zr) + Zr(Ni)	Ni,Zr	a	−8834.3775	2.1706	−8882.2001	2.1335
v(Ni) + i(Ni)	Ni	Fr	−8833.8369	2.7112	−8881.8313	2.5023
v(Zr) + i(Zr)	Zr	Fr	−8832.0903	4.4578	−8879.6059	4.7277

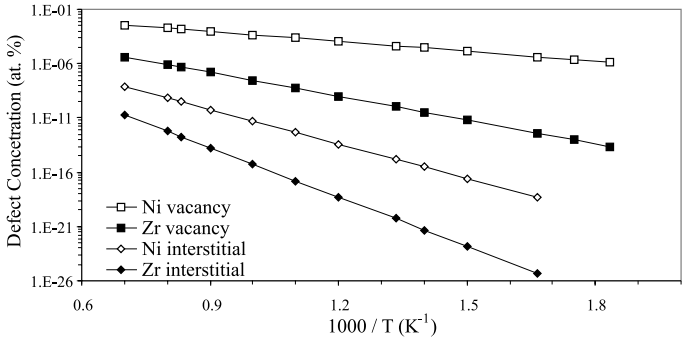

Fig. 2. Arrhenius plots of the concentrations of vacancies and interstitials in Zr_2Ni.

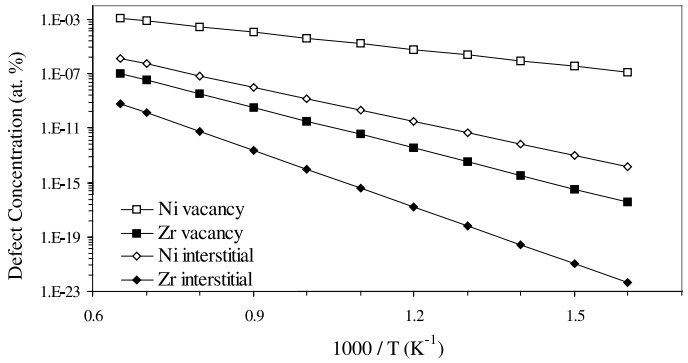

Fig. 3. Arrhenius plots of the concentrations of vacancies and interstitials in ZrNi.

curves. The formation energies for these defects, calculated from the slopes of the corresponding plots, are summarized in Table 2. Since almost all vacancies are in the Ni sublattice, the effective vacancy formation energies are 0.61 and 0.83 eV in the respective compounds. Adapting Hausleitner–Hafner interatomic potentials to the ZrNi compound, Teichler [13] calculated the formation energy of v(Ni) and v(Zr) to be 1.51 and 3.38 eV, respectively. The effect of deviation from stoichiometry was, however, not taken into consideration in these calculations, and the results are clearly much higher than ours. At present, there are no experimental data for comparison with these calculated results; however, it is noted that the interatomic potentials used by Teichler predict a melting temperature that is ~400 K higher than the experimental measurement, whereas the potentials used in the present work underestimate it by ~150 K. Also, for the sake of comparison, it is pointed out that the vacancy formation energy in pure Ni was calculated to be ~1.5 eV [14–16] and experimentally measured to be 1.60–1.80 eV [17,18], while the value measured for pure Zr is 1.75 eV [19]. Likewise, the effective interstitial

Table 2
Effective formation energies (eV)

Defect type	Zr_2Ni	ZrNi
v(Ni)	0.61	0.83
v(Zr)	1.45	1.99
i(Ni)	2.11	1.67
i(Zr)	3.01	2.75
Ni(Zr)	0.61	0.84
Zr(Ni)	1.53	1.38
Ni(Zr) + Zr(Ni)	2.14 (2.17)	2.22 (2.18)
v(Ni) + i(Ni)	2.74 (2.75)	2.50 (2.59)
v(Zr) + i(Zr)	4.48	4.73

formation energies are 2.11 and 1.67 eV in Zr_2Ni and ZrNi, respectively. These values represent roughly half the interstitial formation energy calculated for pure Ni, 4.08 eV [14] or 4.16 eV [15]. The formation energies of antisite defects [Ni(Zr) and Zr(Ni), for Ni occupying Zr site and vice-versa] were also determined in the same manner and their values are also given in Table 2. In both compounds, it is significantly easier to form an Ni-antisite defect, Ni(Zr), than a Zr-antisite defect, Zr(Ni). The formation of antisite pairs $[\mathrm{Ni(Zr)} + \mathrm{Zr(Ni)}]$ and Frenkel pairs $[\mathrm{v(Ni)} + \mathrm{i(Ni)}$ or $\mathrm{v(Zr)} + \mathrm{i(Zr)}]$ does not change the stoichiometry of the system. Therefore, their formation energies were calculated by taking the differences in the total potential energy before and after the defect creation, and are also tabulated in Table 2. As expected, the Frenkel pair formation energy matches perfectly the sum of the interstitial and vacancy formation energies. The same happens for the antisite pairs: their formation energy is equal to the sum of the formation energies of the two individual antisite defects. The values in parentheses were reported earlier by Devanathan et al. [3,4], using the same interatomic potentials. Employing different potentials, Teichler [13] found 2.24, 3.59, and 2.47 and 7.51 eV for the formation energy of Ni(Zr), Zr(Ni), and $[\mathrm{v(Ni)} + \mathrm{i(Ni)}]$ and $[\mathrm{v(Zr)} + \mathrm{i(Zr)}]$ in ZrNi, respectively.

3.2. Vacancy migration mechanisms and energies

Since the stable interstitial configurations are relatively complex, a systematic investigation of interstitial migration has not been undertaken as yet. In the following, we report only the results of our vacancy migration simulations. Moreover, since Zr vacancies are highly unstable and almost all the vacancies are in the Ni sublattice, only the migration of Ni vacancies to neighboring Ni atoms is discussed.

Typical plots of the energy barrier, $E(\eta)$, along the migration path, i.e., $\eta = -1$ to 1, are shown in Figs. 4 and 5. These are for the jump of an Ni vacancy towards a Ni atom in the [0 0 1] and [1 0 0] direction in Zr_2Ni and ZrNi, respectively. The ground state at $\eta = -1$ and $\eta = 1$ is simply the minimum total potential energy when the vacancy

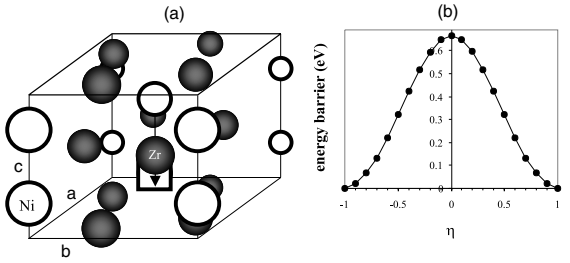

Fig. 4. (a) Crystal structure of Zr_2Ni and (b) energy barrier for the migration of an Ni atom toward a vacancy in the [0 0 1] direction.

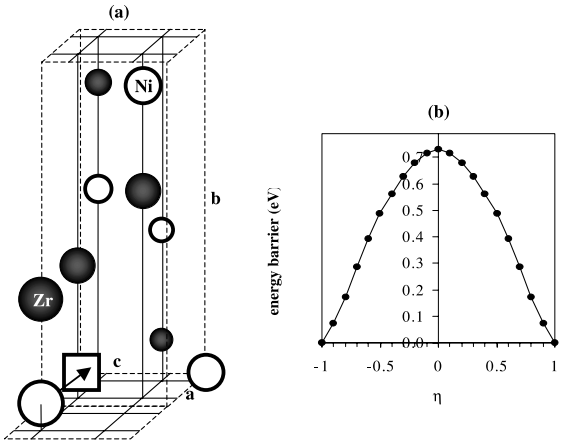

Fig. 5. (a) Crystal structure of ZrNi and (b) energy barrier for the migration of an Ni atom toward a vacancy in the [1 0 0] direction.

(or jumping atom) is at its stable lattice rest position. The maximum value of $E(\eta)$ defines the saddle-point energy, which is the energy that the vacancy must acquire in order to jump to a nearest-neighbor site.

Tables 3 and 4 summarize the vacancy migration energies obtained for different jump directions and jump distances in Zr_2Ni and ZrNi, respectively. In the former compound (Table 3), the vacancy migrates easily by exchanging with nearest-neighbor Ni atoms along the [0 0 1] direction, with a migration energy of 0.67 eV. This type of motion is thus one-dimensional and does not involve any antisite defect formation. Direct

Table 3
Vacancy migration in Zr_2Ni

Direction	Saddle-point energy (eV)	Jump distance (Å)
[0 0 1]	0.67	2.62
[1 1 0]	2.92	4.45
Ring	1.81	4.50

Table 4
Vacancy migration in ZrNi

Direction	Saddle-point energy (eV)	Jump distance (Å)
[0 2 5]	0.67	2.51
[1 0 0]	0.73	3.22
[1 3 4]	2.46	4.19
[0 0 1]	2.66	4.02
Ring	~2	4.18

vacancy jump to an Ni atom at second-neighbor distance, in the [1 1 0] direction, is highly improbable, requiring an energy of 2.92 eV. However, indirect jumps, i.e., via a ring mechanism, are only slightly less improbable; the migration energy for the complete sequence is 1.81 eV. This indirect process involves transient formation of antisite defects in the intermediate steps. In the ZrNi case (Table 4), the energy for vacancy migration to a nearest-neighbor site (in the [0 2 5] direction) is 0.67 eV, identical to that found for Zr_2Ni. The energies for direct vacancy jumps to Ni sites at second-, third- and fourth-neighbor distances (in the [1 0 0], [0 0 1] and [1 3 4] directions) are 0.73, 2.66 and 2.43 eV, respectively. The difference in migration energy between the [0 2 5] and [1 0 0] directions is small enough that it is likely a significant portion of the jumps will occur in the [1 0 0] direction thus making the migration essentially two-dimensional. There are thus two directions for easy vacancy jumps in this compound, [0 2 5] and [1 0 0]. Therefore, vacancy migration is essentially two-dimensional in fully-ordered ZrNi. Indirect vacancy migration to the third-neighbor site involves a ring mechanism, and requires an energy of about 2 eV.

Chemical disorder can greatly decrease the vacancy migration energy and also change the anisotropy of migration. In fact, as shown in Figs. 6 and 7, the vacancy migration energy in both compounds drops significantly if a few Ni antisite defects are present in the nearest neighbor Zr position. In Zr_2Ni (Fig. 6), for example, the Ni vacancy migration energy in the [1 1 0] and [0 0 1] directions decreases by a factor of three Ni antisites are introduced into the Zr sublattice positions that are nearest-neighbors to the migrating vacancy. Nearest-neighbor jumps become very fast, with a migration energy of ~0.2 eV. The migration energy for direct vacancy jumps to second-neighbor Ni sites (in the [1 1 0] direction) is also decreased, requiring only ~0.9 eV. In ZrNi (Fig. 7), on the other hand, four Ni antisite defects must be

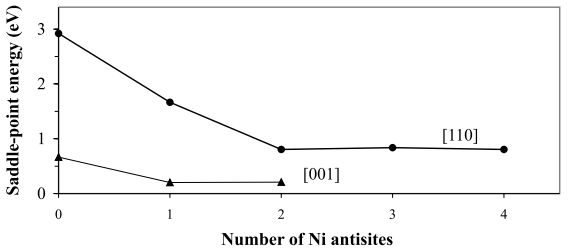

Fig. 6. Saddle point energy for Ni vacancy migration in Zr_2Ni as a function of the number of Ni(Zr) defects placed nearest-neighbor to the migrating vacancy. The top curve corresponds to vacancy migration in the [1 1 0] direction while the bottom curve corresponds to the vacancy migration in the [0 0 1] direction.

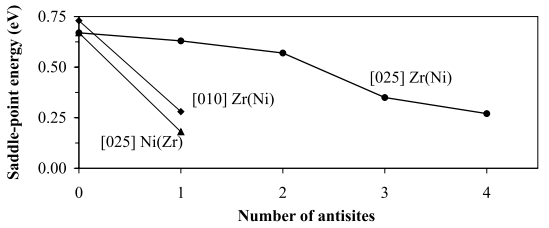

Fig. 7. Saddle-point energy for Ni vacancy migration in ZrNi as a function of the number of different antisite defects placed in nearest-neighbor positions to the migrating vacancy. The various curves correspond to Ni vacancy migration in the $[hkl]$ directions when the indicated antisite defect is introduced nearest-neighbor to the migrating vacancy.

present near the vacancy in order to induce a factor-of-three drop in the energy for vacancy migration to a first-nearest-neighbor Ni site in the [0 2 5] direction. Jumps in the [0 1 0] direction toward second-nearest-neighbor sites are, however, already much faster – with a factor-of-three decrease in energy – even with only one antisite defect in the close vicinity. The presence of Ni antisite defects thus facilitates three-dimensional motion of vacancies in both compounds.

4. Conclusions

In the present work, the properties of atomic defects (i.e., stable configurations, formation and migration energies, and migration mechanisms) in the intermetallic compounds ZrNi and Zr_2Ni have been investigated using molecular-dynamics and molecular-statics simulations. Vacancies are most stable in the Ni sublattice, with formation energies of 0.83 and 0.61 eV in ZrNi and Zr_2Ni, respectively. Zr vacancies are unstable in both compounds, spontaneously decaying to pairs of Ni vacancy and antisite defect. The Zr interstitials are also unstable; they convert to Ni interstitials and antisite defects. In fully-ordered ZrNi, vacancies migrate rapidly in the [0 2 5] and [1 0 0] directions, with migration energy of 0.67 and 0.73 eV, respectively.

Vacancy migration is thus practically two-dimensional. In fully-ordered Zr_2Ni, on the other hand, the vacancy migration is one-dimensional, taking place in the [0 0 1] direction, with a migration energy of 0.67 eV. In both compounds, the presence of antisite defects decreases the vacancy migration energy by up to a factor of three, and facilitates three-dimensional motion.

Acknowledgements

This research was supported by the National Science Foundation, under grant # INT-9503934, by the Brazilian National Research Council, CNPq, and by the Coordination for The Improvement Higher Education Personnel, CAPES.

References

[1] A.T. Motta, J. Nucl. Mater. 244 (1997) 227.
[2] G. Xu, M. Meshii, P.R. Okamoto, L.E. Rehn, J. Alloys Compounds 194 (1993) 401.
[3] R. Devanathan, N.Q. Lam, P.R. Okamoto, M. Meshii, Phys. Rev. B 48 (1993) 42.
[4] R. Devanathan, N.Q. Lam, P.R. Okamoto, M.J. Sabochick, M. Meshii, J. Alloys Compounds 194 (1993) 447.
[5] M.S. Daw, M.I. Baskes, Phys. Rev. B 29 (1984) 6443.
[6] D.J. Oh, R.A. Johnson, J. Mater. Res. 3 (1988) 471.
[7] M.J. Sabochick, S. Yip, J. Phys. F: Met. Phys. 18 (1988) 1689.
[8] M.J. Sabochick, D.L. Richlin, Phys. Rev. B 37 (1988) 10846.
[9] D.O. Welch, G.J. Dienes, O.W. Lazareth, R.D. Hatcher, J. Phys. Chem. Solids 45 (1984) 1225.
[10] S.M. Foiles, M.S. Daw, J. Mater. Res. 2 (1987) 5.
[11] J.R. Shoemaker, R.T. Lutton, D. Wesley, W.R. Wharton, M.L. Oehrli, M.S. Herte, M.J. Sabochick, N.Q. Lam, J. Mater. Res. 6 (1991) 473.
[12] D.A. Porter, K.E. Easterling, Phase Transformations in Metals and Alloys, 2nd Ed., Chapman and Hall, London, 1992, p. 14.
[13] H. Teichler, Phys. Rev. B 59 (1999) 8473.
[14] R.A. Johnson, Phys. Rev. 152 (1966) 629.
[15] N.Q. Lam, L. Dagens, J. Phys. F: Met. Phys. 16 (1986) 1373.
[16] M.I. Baskes, Phys. Rev. B 46 (1992) 2727.
[17] W. Wycisk, M. Feller-Kniepmeier, Phys. Stat. Sol. (a) 37 (1976) 183.
[18] R.W. Siegel, in: J. Takamura et al. (Eds.), Point Defects and Defect Interactions in Metals, University of Tokyo Press, Tokyo, 1982, p. 533.
[19] T. Górecki, Z. Metallkd. 65 (1974) 426.